Astron. Astrophys. 326, 736–740 (1997)

ASTRONOMY AND ASTROPHYSICS

Accuracy of effective temperatures of solar chemical composition stars derived from the flux fitting method

M.L. Malagnini[1] **and C. Morossi**[2]

[1] Dipartimento di Astronomia, Università degli Studi di Trieste, Via G.B. Tiepolo, 11, I-34131 Trieste, Italy
[2] Osservatorio Astronomico di Trieste, Via G.B. Tiepolo, 11, I-34131 Trieste, Italy

Received 8 April 1997 / Accepted 20 May 1997

Abstract. We discuss the uncertainties affecting the determinations of effective temperature and apparent angular diameters based on the flux fitting method. We use Kurucz model fluxes and the spectrophotometric scans given in Breger Catalog. In particular, we analyze and discuss the influence of indetermination which may affect the fixed secondary parameters (i.e. surface gravity, overall metallicity, and interstellar reddening correction) on the estimates of the fitted parameters, $T_{\rm eff}$ and ϕ. The role of different sources of data for the same star and of each of the above mentioned parameters is described in detail for five representative stars, while 130 non–supergiant solar chemical composition stars, in the spectral range G8 – B0, are used to quantitatively illustrate the statistical behaviour of uncertainties.

Key words: stars: general – atmospheres – fundamental parameters

1. Introduction

The availability of new and efficient instrumentation coupled with improved theoretical tools (in particular the technique of synthetic spectra) increases greatly the number of stars for which detailed chemical analyses from high resolution (HiRes) spectra can be performed. As an example, the catalogue by Cayrel et al. (1992; "1991–Catalogue"), contains 3252 $[Fe/H]$ determinations from HiRes for 1676 stars, and both these figures are expected to increase quickly due to the advent of new generation telescopes and spectrographs.

Unfortunately, HiRes observations cover, with very few exceptions, a limited wavelength range, thus preventing accurate and self–consistent determinations of the complete set of fundamental parameters of the stellar photospheres (i.e. effective temperature, surface gravity, elemental chemical abundancies and overall metallicity). In general, values for one or more parameters are taken from different sources estimates, e.g. it is common practice to use effective temperature estimates from the literature or to derive them from the spectral energy distribution (or from calibrations of colours and/or colour indices). Since the quality of HiRes derived gravity and abundancies depends upon the quality of the assumed effective temperature, it is mandatory to carefully analyze the uncertainties affecting the estimates of this fundamental parameter.

In this paper, we discuss and analyze the possible causes and the order of magnitude of the uncertainties affecting the effective temperature values that are derived by applying the flux fitting method. This method is one of the fundamental tools for producing accurate stellar effective temperature determinations. Ideally, one should obtain from the analysis of the spectral energy distributions, at the same time, reliable estimates of effective temperature, surface gravity, overall metallicity, apparent angular diameter and interstellar reddening. Unfortunately, the bulk of observational data has not enough resolution and/or wavelength coverage and/or accuracy and sensitivity for achieving such a goal. Therefore, in general, one or more parameters are given a priori estimates based on collateral information (for instance, log g from spectral classification). Thus, careful investigation on the possible (systematic) uncertainties affecting the derived $T_{\rm eff}$, because of indetermination in the values of the fixed secondary parameters, is fundamental.

In Sect. 2 we describe the observational data (spectrophotometric scans from Breger Catalog, 1976b) and the theoretical framework of Kurucz model fluxes (Kurucz, 1993; hereafter K93). Sect. 3 describes the basic steps of the flux fitting, and Sect. 4 presents our results on the uncertainties affecting the derived effective temperature and apparent angular diameter estimates.

2. Input data

2.1. The observational database

Visual spectrophotometric data are from Breger catalog (Breger, 1976b). This catalog contains an extensive and homogeneous collection of ground–based stellar observations of continuum or pseudo–continuum regions (35 at maximum) in the wavelength

Send offprint requests to: M.L. Malagnini

range 3200–10,000 Å. For some stars, multiple entries are available, referring to different observational sources, wavelength coverage and sampling.

The stars discussed in this paper were selected according to the following criteria: spectral types G8 – B0; luminosity classes III to V; no anomalies and/or peculiarities reported in Jascheck & Egret (1982). Luminosity classes II to Ia were excluded since K93 models are based on the plane parallel and LTE approximations which are expected to be inadequate for these categories of objects. The selection produced a list of 302 stars, for which 437 different sets of observational data are available. Each set is treated independently.

The spectrophotometric scans were de–normalized using the visual magnitude values and converted to the same absolute flux scale, according to the specifications reported in Breger catalog, and then re–scaled to Hayes (1985) Vega spectral energy distribution.

2.2. The theoretical database

The observed absolute fluxes are fitted to a grid of theoretical flux spectra computed from model atmospheres. The grid was computed by Kurucz with ATLAS9, a model atmosphere program which takes into account up–to–date line and continuous opacities, including a list of over 58 millions of atomic and molecular lines.

The fluxes are predicted at 1221 wavelengths, in the wavelength range from 90 Å to 1,600,000 Å, with samplings on the order of 10 Å in the ultraviolet, up to 50 Å in the visual region, and increasing further in the infrared.

The theoretical fluxes are re–sampled for matching the wavelength sampling of each different spectrophotometric scan, and fitted to the observational data as described in Malagnini & Morossi (1983,1990).

3. Method of the analysis

We perform the fit of stellar spectral data with theoretical fluxes by applying a least–mean–square–error criterion in order to derive simultaneously stellar effective temperatures ($T_{\rm eff}$) and apparent angular diameters (ϕ). Before applying the fitting procedure, each set of stellar data is applied an interstellar reddening correction, by assuming a reddening law and the appropriate $E(B-V)$ value. From among the K93 grid, a subset of theoretical spectra is selected, according to the proper values for the metallicity ($[M/H]$) and surface gravity ($\log g$) of the program stars. Since the stars are assumed to be of solar chemical composition, we start with the grid of spectra computed for $[M/H] = 0.0$. As far as $\log g$ is concerned, each star is assigned a value according to its spectral classification.

In order to quantify the influence of uncertainties affecting the values assumed for the parameters $[M/H]$, $\log g$ and $E(B-V)$ on the estimates of $T_{\rm eff}$ and ϕ, we proceed as described in the following subsections.

3.1. Reddening

In the case of reddened stars, the model flux distributions were modified, before performing the fit, according to Nandy et al. (1975). No significant differences were observed when using Mathis law (1990) instead, providing that the two laws are re–normalized to the same visual extinction parameter.

The reddening color excesses were estimated by comparing the $(B-V)_{\rm o}$ value expected for each star according to its spectral class (FitzGerald, 1970) with the observed $(B-V)$ color. Since an uncertainty of ± 0.02 mag in $E(B-V)$ can be reasonably expected, the fit was performed three times for each observational data set, by using the nominal $E(B-V)_{\rm nom}$ and the two extreme cases, $E(B-V)_{\rm nom} \pm 0.02$ mag.

3.2. Metallicity

The program stars were selected to represent solar chemical composition objects and information on metallicity has been checked by using the 1991–Catalogue. In general, $[Fe/H]$ determinations are consistent with the hypothesis of solar chemical composition. However, deviations as large as ± 0.5 dex were found for some stars or for individual estimates for the same star. Therefore, assuming an uncertainty on $[M/H]$ of ± 0.5 dex, we used the three subsets of K93 grid at $[M/H] = -0.5, 0.0, 0.5$ dex as theoretical input.

3.3. Surface gravity

A nominal value for the surface gravity was fixed according to the stellar spectral classification. To be conservative, we assumed that the "true" $\log g$ may differ by ± 0.5 dex from the assigned value, and the fit was performed three times for each data set, by using the nominal $\log g_{\rm nom}$ and the two extreme cases ($\log g_{\rm nom} \pm 0.5$).

4. Results and discussion

In principle, for each of the 437 sets of observational data available, we expect 27 solutions ($T_{\rm eff}$, ϕ), one for each combination of the secondary parameters, ($[M/H]$, $\log g$, $E(B-V)$). To select the solutions consistent with the accuracy of the observations, we adopt a threshold on the RMSE of the fit. By taking into account the observational errors reported in Breger(1976a), we fix an acceptance threshold of 0.025 mag.

One should obtain estimates of all the unknown parameters, and not only ($T_{\rm eff}$, ϕ), by identifying the "best" solution, i.e. the one with the minimum value of the RMSE of the fit. This would happen if the data carry on the proper relevant signatures, but this is not the case of the generally available spectral energy distribution data. The spectrophotometric scans have characteristics much looser than those required to meet the requirements, therefore they may be compatible with more than one set of parameters.

It results that, out of the 302 program stars, 202 have a number of acceptable solutions varying from one up to over 100 for the same star, by considering all together solutions coming

Table 1. Basic data, nominal values of secondary parameters and results for five representative stars

HD	SP class	V mag	$B-V$ mag	$E(B-V)_{\rm nom}$ mag	log $g_{\rm nom}$	$N_{\rm sol}$	$T_{\rm eff}$ K	$\Delta T_{\rm eff}$ K	ϕ marcsec	$\Delta\phi$ marcsec
74575	B1.5 III	3.68	-0.18	0.07	4.0	53	22857	1046	0.304	0.007
102647	A3 Vv	2.14	0.09	0.01	4.0	38	8857	185	1.374	0.033
160762	B3 VSB	3.80	-0.18	0.02	4.0	48	16597	497	0.346	0.006
188350	A0 III	5.61	0.10	0.13	3.5	81	9637	118	0.292	0.007
214923	B8.5 V	3.40	-0.09	0.02	4.0	104	11218	124	0.587	0.009

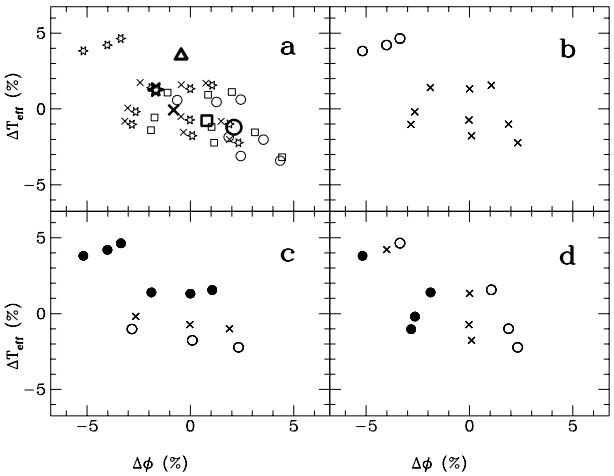

Fig. 1a–d. Displacements ($\Delta\phi$, $\Delta T_{\rm eff}$) of individual solutions from the average values for HD 102647 (see Table 1): **a** results for five observational datasets, each marked by a different symbol (bold symbols refer to the mean displacements of each dataset), **b** subset of the results (only one dataset is plotted) referring to solutions (if any) with different values of surface gravity, i.e. the nominal value (crosses), log $g_{\rm nom}$ + 0.5 (filled circles), and log $g_{\rm nom}$ − 0.5 (open circles), **c** as in **b** for solutions (if any) with different values of color excess, i.e. the nominal value (crosses), $E(B-V)_{\rm nom}$ + 0.02 mag (filled circles), and $E(B-V)_{\rm nom}$ − 0.02 mag (open circles), **d** as in **b** for solutions (if any) with different values of overall abundance, i.e. the nominal value (crosses), $[M/H]_{\rm nom}$ + 0.5 (filled circles), and $[M/H]_{\rm nom}$ − 0.5(open circles)

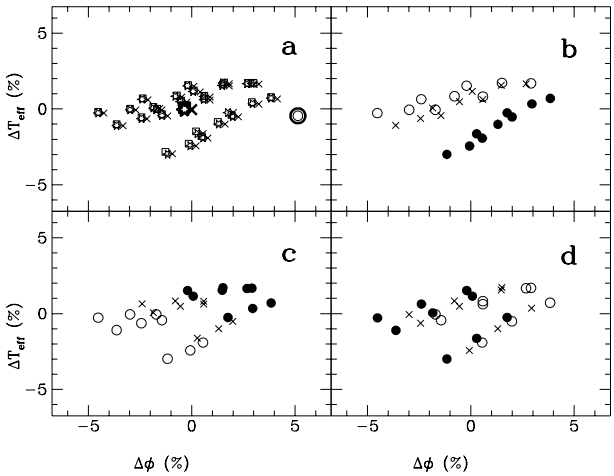

Fig. 2a–d. Same as Fig. 1 for HD 188350

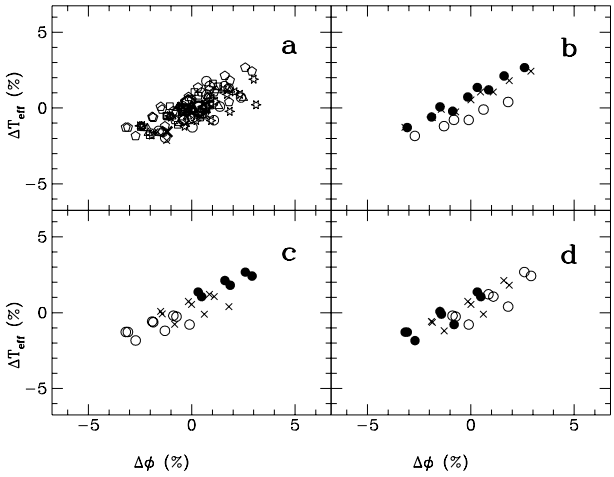

Fig. 3a–d. Same as Fig. 1 for HD 214923

from different observational sets. While the problem of choosing the most appropriate (if any) solution for each star will be faced in a forthcoming paper which will also present comparisons with determinations from other methods, in this paper we focus our attention on the uncertainties induced by the indetermination of the fixed secondary parameters. In the following, in order to make statistically significant inferences, we limit our analyses to the 130 stars for which at least ten solutions are available.

First of all, let us discuss into details the behaviour of the solutions for five stars of different spectral classifications, selected because of the high number of solutions.

Figs. 1 to 5 show, in the plane (ϕ, $T_{\rm eff}$), the solutions for the five representative stars (ordered according to increasing stellar effective temperature) for which basic information is provided in Table 1. In each figure, the four panels illustrate the role of the four causes of uncertainties taken into account: i.e. discrepancies among different observational sources (panel **a**), indetermination in the values of log g (panel **b**), $E(B-V)$ (panel **c**), and $[M/H]$ (panel **d**). The symbols represent the percentage displacements of individual results from the average (ϕ, $T_{\rm eff}$) values computed over the total number of solutions ($N_{\rm sol}$) referring to each star (Table 1, columns 7, 8 and 10). In panel **a** different symbols represent different datasets, and bold symbols mark the average displacements computed for each dataset.

The other three panels contain the results pertaining to the dataset with the highest number of solutions. The role of the dif-

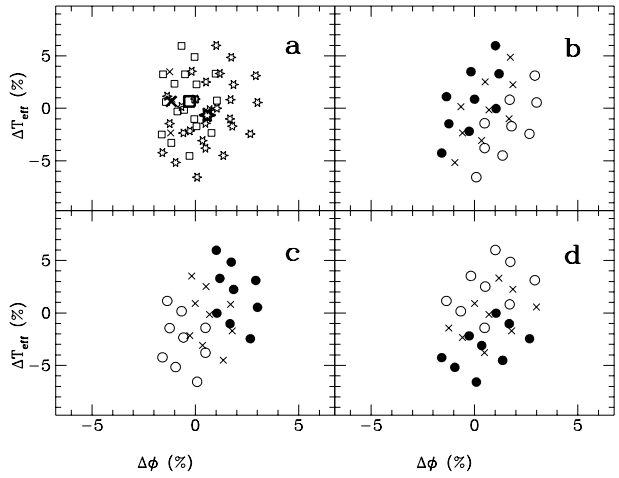

Fig. 4a–d. Same as Fig. 1 for HD 160762

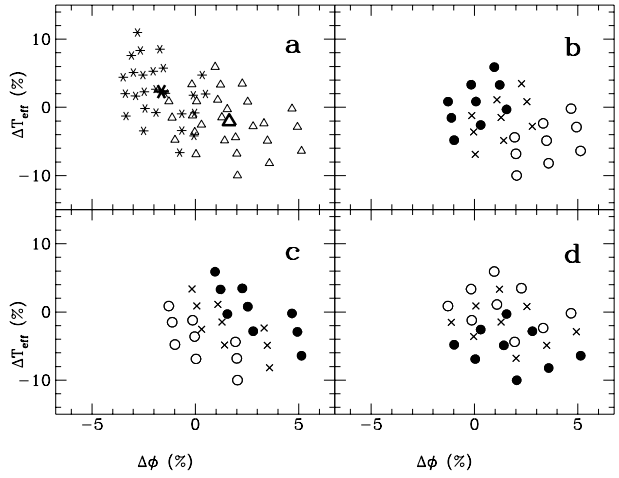

Fig. 5a–d. Same as Fig. 1 for HD 74575

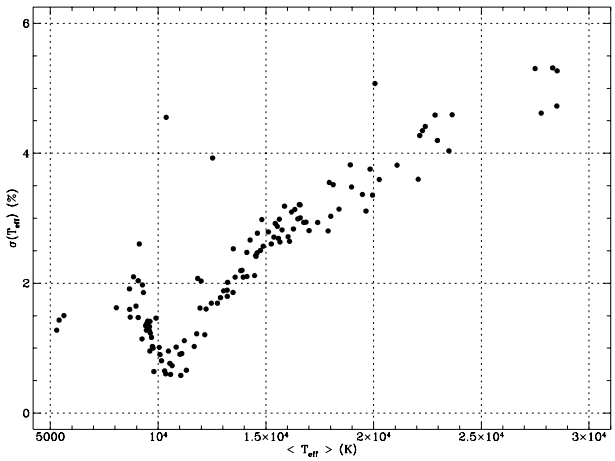

Fig. 6. Percentage dispersion, $\sigma(T_{\rm eff})$, versus average effective temperatures, $< T_{\rm eff} >$, for the 130 stars with ten or more solutions

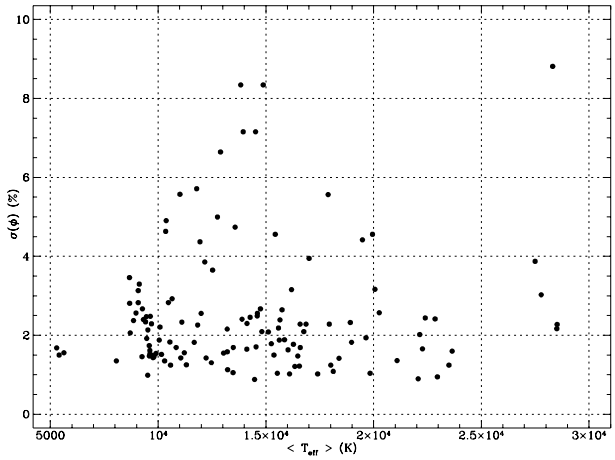

Fig. 7. Percentage dispersion, $\sigma(\phi)$, versus average effective temperatures, $< T_{\rm eff} >$, for the 130 stars with ten or more solutions

ferent choices for each of the 3 unfitted parameters is depicted by using different symbols: results referring to the nominal values are marked by crosses, while those referring to the maximum and minimum value of the parameters are marked by filled and open symbols, respectively.

In all the five cases the spread of the solutions in $\Delta\phi$ is confined within $\pm 5\%$, by taking into account different sources (panel **a**) and/or different values of the secondary parameters ($\log g$ in **b**, $E(B-V)$ in **c**, and $[M/H]$ in **d**). While the use of different data sources produce results often systematically different from one source to another (see in particular Figs. 4, 5), the behaviour with respect to the other parameters is almost source–independent. Therefore, in each figure panel **a**) refer to all the available source, while the other panels refer, for each star, only to the source for which the highest number of solutions is available.

Figs. 1–3 show a spread in $\Delta T_{\rm eff}$ on the same order of $\Delta\phi$, while Figs. 4 and 5 show higher dispersion. For the two cooler stars (Figs. 1, 2) the solutions characterized by the use of the lower value for $\log g$ have higher temperatures and slightly lower angular diameters than those corresponding to $\log g_{\rm nom}$. The hotter stars present an opposite trend. By using $\log g_{\rm nom} + 0.5$, no solutions are obtained for HD 102647, while the above described behaviour is confirmed for the other stars. In all the cases the use of the upper value for $E(B-V)$ reflects in an increase in $T_{\rm eff}$ and in ϕ, but for HD 102647. The role of $[M/H]$ is not so clear, even if a tendency to a decrease in temperature with increasing metallicity can be seen for the stars at higher temperatures.

Coming now to the analysis of the 130 stars with more then ten solutions, we study in a more general way the global uncertainties affecting the solutions. Since all the solutions are equivalent in the sense of the full consistency of the RMSE of the fit with the observational accuracies, we computed for each star the average values and standard deviations of $T_{\rm eff}$ and ϕ.

Fig. 6 shows the percentage dispersion in $T_{\rm eff}$ versus the average effective temperature. Apart from few outliers, the points indicate a well defined trend of the dispersion versus $< T_{\rm eff} >$ with a minimum around 10,000 K. The percentage dispersion ranges from 0.6% up to 5.3%.

Fig. 7 shows the percentage dispersion in ϕ versus the average effective temperature. There is no trend and the percentage dispersion ranges from 1.0% up to 8.9% with the bulk of the data clustered around 2.0%.

There is neither a correlation between each one of the two percentage standard deviations with the average apparent angular diameter nor between them.

To check the soundness of the assumed nominal values of the fixed secondary parameters, we averaged for each star the values of $[M/H]$, $\log\ g$, and $E(B-V)$ of the solutions and we obtained the following results:

1. All the stars have solutions consistent with the starting hypothesis of solar chemical composition since their $[M/H]$ average values fall in the range ± 0.25 dex.
2. There are only 8% of the cases with an average value of $\log\ g$ which differs by more than ± 0.25 dex from the nominal value;
3. As far as $E(B-V)$ is concerned, in 83% of the cases the average color excesses are consistent (within $\pm$ 0.01 mag) with the nominal ones;
4. 95 out of 130 stars (73%) have solutions which, as a whole, are fully consistent with the assumed values of the secondary parameters.

In conclusion, by using the flux fitting method, the indetermination in the values of the fixed secondary parameters reflects into uncertainties in the determinations of $T_{\rm eff}$ and ϕ on the order of 2% (median values), spanning the ranges 0.6–5.3% and 1–9%, respectively. These uncertainties must be taken into account by those scientists who use these effective temperatures in their analyses of HiRes spectra in order to avoid systematic errors in their results on chemical abundancies of individual elements.

Acknowledgements. This work was partially supported by the Italian MURST (60% and 40% grants, Università degli Studi di Trieste, and Osservatorio Astronomico di Trieste), and by the Consiglio Nazionale delle Ricerche (CNR–GNA).

References

Breger, M. 1976a, ApJS, 32, 1
Breger, M. 1976b, ApJS, 32, 7
Cayrel de Strobel, G., Hauck, B., François, P., Thévenin, F., Friel, E., Mermilliod, M., and Borde, S. 1992, A&AS, 95, 273 (1991–Catalogue)
FitzGerald, M.P. 1970, A& A, 4, 234
Jaschek, M., Egret, D.: 1982, Catalogue of Stellar Groups, Publication Spécial du C.D.S., No. 4
Hayes, D.S. 1985, Calibration of Fundamental Stellar Quantities, IAU Symposium no. 111, D.S. Hayes, L.E. Pasinetti and A.G.D. Philip, Dordrecht: Reidel, 225
Kurucz, R. L. 1993, CD–ROM 13, ATLAS9 Stellar Atmosphere Programs and 2 km/s Grid (Cambridge: Smithsonian Astrophys. Obs.) (K93)
Malagnini, M.L., Morossi, C. 1983, Statistical Methods in Astronomy, ESA SP–201, 27
Malagnini, M.L., Morossi, C. 1990, A&AS, 85, 1015
Mathis, J.S. 1990, ARA&A, 28, 337
Nandy, K., Thompson, G.I., Jamar, C., Monfils, A., and Wilson, R. 1975, A& A, 44, 195

This article was processed by the author using Springer-Verlag LaTeX A&A style file *L-AA* version 3.